Infrared Physics & Technology 70 (2015) 15–19

Contents lists available at ScienceDirect

Infrared Physics & Technology

journal homepage: www.elsevier.com/locate/infrared

InAs/GaAs quantum dot and dots-in-well infrared photodetectors based on *p*-type valence-band intersublevel transitions

A.G. Unil Perera [a,*], Yan-Feng Lao [a], Seyoum Wolde [a], Y.H. Zhang [b], T.M. Wang [b], J.O. Kim [c], Ted Schuler-Sandy [c], Zhao-Bing Tian [c], S.S. Krishna [c]

[a] Department of Physics and Astronomy, Georgia State University, Atlanta, GA 30303, USA
[b] Key Laboratory of Artificial Structures and Quantum Control, Department of Physics and Astronomy, Shanghai Jiao Tong University, Shanghai 200240, China
[c] Center for High Technology Materials, Department of Electrical and Computer Engineering, University of New Mexico, Albuquerque, NM 87106, USA

HIGHLIGHTS

- We demonstrate high quantum efficiency (17%) InAs/GaAs *p*-type quantum dot infrared photodetector.
- The *p*-type hole response displays a well-preserved spectral profile, independent of the applied bias.
- The *p*-type quantum dot photodetector exhibits a strong far-infrared response up to 70 μm.

ARTICLE INFO

Article history:
Received 16 July 2014
Available online 5 November 2014

Keywords:
Photodetectors
Quantum dots
Quantum wells

ABSTRACT

InAs/GaAs quantum dot (QD) and dots-in-well (DWELL) infrared photodetector (QDIP) based on *p*-type - valence-band intersublevel hole transitions are reported. Two response bands observed at 1.5–3 and 3–10 μm are due to optical transitions from the heavy-hole to spin–orbit split-off QD level and from the heavy-hole to heavy-hole level, respectively. The *p*-type hole response displays a well-preserved spectral profile (independent of the applied bias) observed in both QD and DWELL detectors. At elevated temperatures between 100 and 130 K, the DWELL detector exhibits a strong far-infrared responses up to 70 μm. An external quantum efficiency of 17% is demonstrated. The studies show the promise of *p*-type QDs for developing infrared photodetectors.

1. Introduction

The quantum dot infrared photodetector (QDIP) has received considerable attention, owing to the advantage of three-dimensional confinement of carriers [1]. Widely studied *n*-type QDIPs and dots-in-well (DWELL) detectors are featured with the characteristics of multicolor and bias selectivity [2,3]. The optimized bound-to-bound transitions in a GaAs-based *n*-type DWELL structure has led to the achievement of 12% QE [4]. Most of studies have focused on the operation based on *n*-type electrons [5,4]. Despite the promising characteristics, a major challenge associated with QDIPs is the low quantum efficiency (QE) [6]. The relatively low QE of QDIPs results in part from the large fluctuation of the dot size in the Stranski–Krastanov growth mode. This, along with the low QD density as compared to the density of dopants in quantum-well infrared photodetectors (QWIPs), gives rise to the lower absorption efficiency than expected. Photodetectors based on *p*-type doping are not studied as widely as the *n*-type counterpart. Room-temperature operation by utilizing *p*-type inter-valence-band transitions [7–9] were recently demonstrated using bulk heterojunctions. Aside from the high-temperature operation, inter-valence-band transitions typically yield a broad-band absorption and detection spanning from 1 μm up to beyond 10 μm [10]. This allows for a convenient tuning of the spectral response by adjusting the heterojunction band offset. However, an intrinsic drawback of using bulk semiconductors is the fast carrier relaxation time, which is, for example, about 0.1 ps for $1 \times 19\ cm^{-3}$ *p*-type doped GaAs. In contrast, quantum structures such as dots or dots-in-well are demonstrated to have longer lifetime of photocarriers (up to nanoseconds) [11]. As such, an integration of the QD structure and *p*-type hole transitions could offer an alternative route to develop high performance QDIPs.

In this article, we discuss *p*-type InAs/GaAs QDIP [12] and DWELL [13] detectors, operating based on the valence-band intersublevel hole transitions. The use of *p*-type hole response shows promising characteristics; for example, a quantum efficiency of

* Corresponding author.
E-mail address: uperera@gsu.edu (A.G. Unil Perera).

http://dx.doi.org/10.1016/j.infrared.2014.10.016
1350-4495/

17% is demonstrated. Additionally, hole response has a well-preserved spectral profile, as opposed to conventional *n*-type electron response strongly dependent on applied bias. Operation based on holes involves optical transitions associated with three valence bands (VBs) and higher effective mass of the holes. The former leads to a broad response allowing for convenient tailoring of the spectral response. The latter features increased density of states and thus enhanced absorption, as a great number of holes are allowed in QDs. Also, higher effective mass of holes means the lower dark current compared to conduction through electrons.

2. Device structures

The *p*-type QDIP and DWELL structures are grown by molecular beam epitaxy, as shown in Fig. 1(a) and (b), respectively [12,13]. The absorbing region consists of 10 periods of InAs QDs, between which is an 80-nm thick undoped GaAs layer. For the DWELL structure, QD layers are embedded in a 6-nm thick $In_{0.15}Ga_{0.85}As$ QWs. The pyramidal shape of QDs has the height and base dimensions of ~ 5 and $\sim$20–25 nm, respectively. The dot density is about 5×10^{10} cm^{-2}. Free holes are introduced by a δ-doping technique. A sheet density of 5×10^{11} cm^{-2} *p*-type dopants is placed above the QDs, with a 15-nm thick spacer (GaAs) in-between them, which gives about 10 holes per dot.

The detectors were processed by wet etching to produce square mesas, which was followed by evaporation of Ti/Pt/Au ohmic contacts onto the top and bottom *p*-type GaAs contact layers. A top ring contact with a window opened in the center was fabricated to allow front-side illumination. The experiments were carried out on 400×400 μm^2 mesas with an open area of 260×260 μm^2 in the center allowing for front-side illumination. A Perkin–Elmer system 2000 Fourier transform infrared spectrometer is used to measure the spectral response. A bolometer with known sensitivity is used for background measurements and calibration of the responsivity.

3. Results and discussion

The electronic structures of QDIP and DWELL detectors are shown in Fig. 1(c) and (d). In contrast to only one electron state in the conduction band, many hole states are allowed in the dots. From numerical computation point of view, this means a massive number of eigenvalues to be solved simultaneously from the

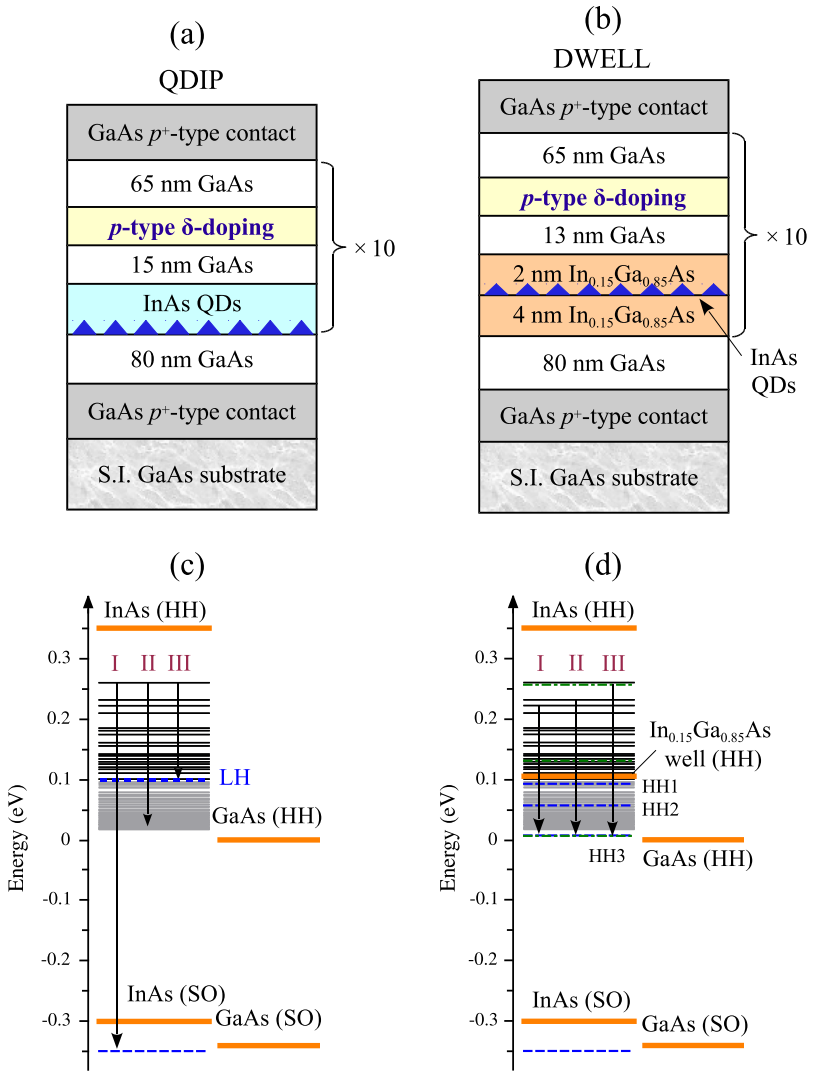

Fig. 1. Schematics of the *p*-type (a) QDIP and (b) DWELL structures. Free holes are introduced into QDs by δ-doping above the QD layer. (c) and (d) are the computed valence band structures of the QDIP and DWELL detectors, respectively, where solid horizontal lines represent for hole states obtained by using an 8×8 $\boldsymbol{k} \cdot \boldsymbol{p}$ model [16]. The thick lines are the band edges. The dashed lines are the calculated using an effective-mass method. The labeled HH1–HH3 are the levels of the $In_{0.15}Ga_{0.85}As$/GaAs QW [13]. Indicated transitions agree with the experimental response.

eight-band Hamiltonian, which becomes even difficult in the higher hole energy range where dense states are included. To facilitate the computation, the spin–orbit split-off (SO) states were obtained by treating the QD as a quantum well (QW) and using an effective-mass method. The much wider in-plane dimension of the dots than the height partially validates such a treatment. We use the QW SO state to represent for the QD SO hole and interpret the spectral response, which should be acceptable for analysis on distinguishing respective contributions of VB hole transitions to the response. The DWELL detector has two sets of energy levels, corresponding to the QD and QW, respectively. The $In_{0.15}Ga_{0.85}As/GaAs$ QW contains three HH levels (dashed lines), which are obtained using an effective-mass method [14].

The dominant response of the *p*-QDIP was observed at 1.5–3 and 3–10 μm, as shown in Fig. 2. The overall spectral profile is analogy with that of the *p*-type GaAs heterojunction detector (inset of Fig. 2). However, the responsivity of *p*-QDIP is about 10–20 times higher than that of the heterojunction detector, despite that QDIP contains a much thinner absorbing region than the heterojunction. This characteristic indicates that the origin of response should be dominantly due to the QDs but not the *p*-type GaAs contact layers, benefiting from the longer hole lifetime of QDs. As shown in the inset of Fig. 2, the response of QDIP is also higher than that of the DWELL detector, owing to the less hole escape probability in the DWELL structure.

The small spacing between hole states (< 30 meV) leads to varying response with the photon energy in accordance with the band structure of InAs/GaAs. For example, the two response bands lie above and below the SO splitting energy of InAs (0.39 eV or 3.2 μm in wavelength) for the *p*-QDIP. The experimental short-wavelength response peak at 0.552 eV corresponds to the hole transition from the HH ground state to the SO state (transition I of Fig. 1(c)), while the long-wavelength peak at 0.247 eV corresponds to the hole transition from the HH ground state to the state near the GaAs barrier (transition II). It was observed that a small long-wavelength response tail rises at higher bias with its peak at 0.148 eV (transition III).

The optical transitions ending up at the bound states (above the GaAs heavy-hole/light-hole (HH/LH) band edge in the valance-band diagram) do not contribute to the response unless photoexcited holes surpass the GaAs barrier. This is expected to be accomplished by a tunneling process, leading to bias-dependent response. However, such a characteristic is not observed in our *p*-type QDIP as well as the *p*-DWELL detector. For comparison at different biases, response spectra are normalized by multiplying a factor, as shown in Fig. 3(a) and (b) for the QDIP and DWELL detectors, respectively, where the insets show two primary

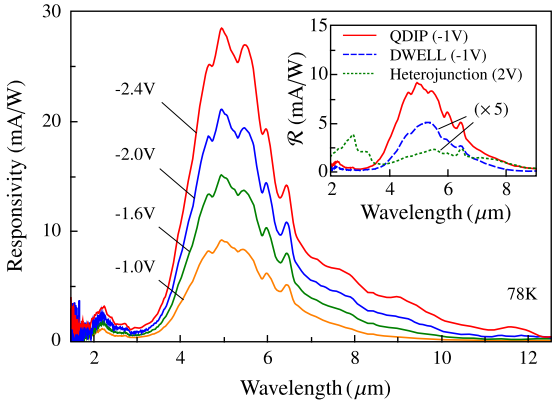

Fig. 2. Spectral response of the *p*-type QDIP at 78 K. Inset: response spectra of the *p*-type QDIP, DWELL and GaAs/AlGaAs heterojunction detectors [9] are compared. The bias voltages are selected such that they lead to nearly the same electric field.

response peaks at 0.1–0.4 eV (3–12 μm) and 0.4–0.8 eV (1–3 μm) due to HH–HH and SO–HH hole transitions, respectively. It can be seen that the spectral response is distinctly different from the *n*-type DWELL detectors [2,4], where the wavelength range of the response varies from the mid-wavelength infrared to long-wavelength infrared. No apparent change in the spectral profile of the response is observed.

To identify individual transitions contributing to the spectral response, Gaussian fittings were carried out. The spectral response of the *p*-type QDIP is dominated by a Gaussian peak at low bias. An additional high-energy peak occurs at high negative bias and is attributed to be due to the HH bound-to-LH bound transition (transition III in Fig. 1 (QDIP)). For the DWELL detector, three peaks can be resolved. Neither of them can be induced or annihilated by changing the bias. This characteristic indicates the trivial influence of the QD bound-to-QW bound transition on the response, as response based on the bound-to-bound transition should be strongly bias dependent as a consequence of the escape of photoexcited holes through tunneling. Much reduced tunneling probability of holes allows an explanation for this feature. Calculation of tunneling probability based on the Wentzel-Kramers-Brillouin (WKB) approximation shows that more than $10^3 - 10^5$ higher tunneling probability of electrons than that of the holes is the reason of bias-dependent response in the *n*-type DWELL detectors, whereas the spectral range of the *p*-type response remains stationary at different biases.

The hole transition which contributes to the primary response peak of *p*-QDIP at 0.247 eV may end up to quasibound states. Hole states becomes denser at the higher energy portion of the HH confinement potential, due in part to the larger hole effective mass and to the LH confinement potential, which leads to a continuum of tenuously bound states [15]. This characteristic is consistent with the broad nature of the response peak with $\Delta\lambda/\lambda = 0.42$, where λ and $\Delta\lambda$ are 5.2 μm and 2.2 μm, respectively. However, the HH bound-to-HH quasibound transition may dominate over the HH bound-to-LH continuum transition, as the bound-to-quasibound transition has the higher absorption than the bound-to-continuum transition. Compared to the HH to HH response, the short-wavelength response peak contributed by the HH to SO transition is not as strong as in the heterojunction case, as shown in Fig. 2. A possible cause is the impact of strain on the local band edges, leading to a much shallower SO confinement potential than the HH band and giving rise to continuum SO states.

By using experimentally measured noise current (i_n), the noise gain (g) can be calculated through the expression: $g = i_n^2/4eI_d$, where I_d is the dark current (Fig. 4(a)). The calculated gain is shown in Fig. 4(b). The value of QE can be obtained using $QE = \mathcal{R} \times hv/eg$, as shown in Fig. 4(c), where $\mathcal{R}$ is the responsivity. The experimental dark current of DWELL is about 40 times less than that of QDIP. The maxim QE of the QDIP and DWELL detector is obtained to be 17% and 9%, respectively. The specific detectivity is given by $D^* = R\sqrt{A \times \Delta f}/i_n$, where A is the device area and Δf is the bandwidth. The maximum values of detectivity at 78 K for the response peak at 5 μm are 1.8×10^9 and 1.4×10^9 cm $Hz^{1/2}$/W, respectively.

It was found that a strong far-infrared responses is observed at higher temperatures (100–130 K), as shown in Fig. 5. As for the normal response peak (<10 μm), its intensity decreases with increasing temperature while the far-infrared response increases with increasing temperature. Thermal excitation of carriers from the ground state to excited states can increase the absorption of the far-infrared radiation (low energy transition), and thus enhance the response. It is confirmed that the far-infrared response appears only at temperatures above ~ 100 K and increases as the temperature rises from 100 K to 130 K. The calculated energy spacing between the dot levels is about 5–28 meV. There is no peak shift with either bias voltage or temperature. From 78 K to 130 K, the peak responsivity of the 5.4 μm peak decreases by ~65%, while

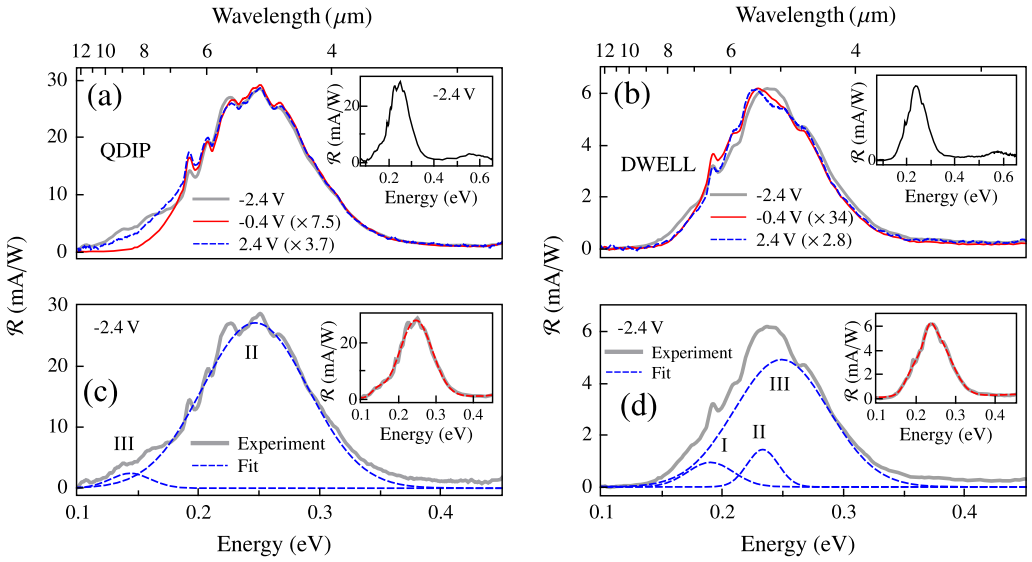

Fig. 3. Normalized spectral response of (a) QDIP and (b) DWELL detectors at 78 K, where the insets plot the whole spectral range including a higher-energy peak. (c) and (d) are Gaussian fittings, where each dotted lines (Gaussian components) gives the observed spectra in (a) and (b). Insets show the summation of the Gaussian components, in good agreement with the experimental spectra.

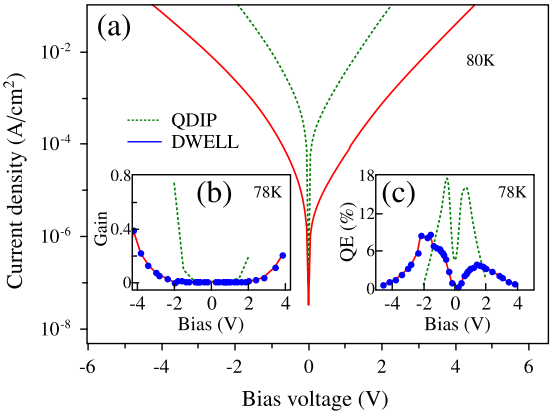

Fig. 4. (a) Dark current density of the *p*-type QDIP and DWELL at 80 K. (b) and (c) (shown as insets) are the gain and QE, respectively.

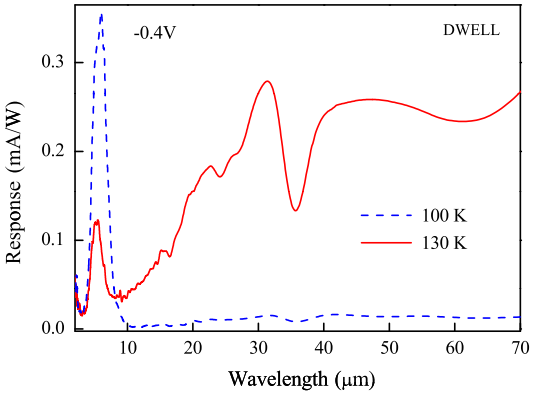

Fig. 5. The far-infrared response observed at high temperatures in the DWELL detector, as a consequence of increasing occupancy of carriers in the high-energy level with increasing temperature.

the far-infrared response around 32.6 μm increases by a factor of ~100.

The demonstrated *p*-type QD detectors do not employ a dark current blocking layer. This causes the dark current more than three orders of magnitudes higher than that of *n*-type QDIPs which typically use a current-blocking layer [3]. Although the current blocking layer also reduces the responsivity, the noise is suppressed more effectively, leading to increased signal to noise ratio and the detectivity [3]. Further improvement of the QE could be accomplished through optimizing the optical transition type, for example, by using bound-to-bound transitions, which should lead to improvement in the absorption.

4. Conclusions

To conclude, we have demonstrated the promise of using *p*-type hole transitions to develop QDIPs, with a higher QE of 17% being demonstrated. Two response bands at 1.5–3 and 3–10 μm were confirmed as being due to hole transitions from the HH to SO level and from the HH to HH level, respectively. The DWELL detector displays constant wavelength ranges of response independent of applied biases. Its spectral response results from transitions between QD bound states and near-barrier QW states. The well-preserved spectral response should benefit the optimization of bias for optimum response and the control of spectral response for the detector development. Furthermore, a far-infrared response originating from high-temperature operation (100–130 K) is observed in the DWELL detector, as a consequence of transitions between excited QD levels. This allows for the *p*-type QDs to be potentially used to develop high-temperature Terahertz detectors.

Conflict of interest

The authors declare there are no conflict of interests.

Acknowledgment

This work was supported in part by the U.S. National Science Foundation under Grant No. ECCS-1232184.

References

[1] V. Ryzhii, The theory of quantum-dot infrared phototransistors, Semicond. Sci. Technol. 11 (5) (1996) 759.

[2] S. Krishna, S. Raghavan, G. von Winckel, A. Stintz, G. Ariyawansa, S.G. Matsik, A.G.U. Perera, Three-color ($\lambda_{p1} \sim 3.8$ μm, $\lambda_{p2} \sim 8.5$ μm, and $\lambda_{p3} \sim 23.2$ μm) InAs/InGaAs quantum-dots-in-a-well detector, Appl. Phys. Lett. 83 (14) (2003) 2745–2747.
[3] A.V. Barve, S. Krishna, Advances in Infrared Photodetectors (Semiconductors and Semimetal Series)), vol. 84, Elsevier, 2011.
[4] A.V. Barve, T. Rotter, Y. Sharma, S.J. Lee, S.K. Noh, S. Krishna, Systematic study of different transitions in high operating temperature quantum dots in a well photodetectors, Appl. Phys. Lett. 97 (6) (2010) 061105.
[5] G. Ariyawansa, A.G.U. Perera, G. Huang, P. Bhattacharya, Wavelength agile superlattice quantum dot infrared photodetector, Appl. Phys. Lett. 94 (2009) 131109–131110.
[6] A. Rogalski, J. Antoszewski, L. Faraone, Third-generation infrared photodetector arrays, J. Appl. Phys. 105 (9) (2009) 091101.
[7] A.G.U. Perera, S.G. Matsik, P.V.V. Jayaweera, K. Tennakone, H.C. Liu, M. Buchanan, G. Von Winckel, A. Stintz, S. Krishna, High operating temperature split-off band infrared detectors, Appl. Phys. Lett. 89 (13) (2006) 131118–131120.
[8] P.V.V. Jayaweera, S.G. Matsik, A.G.U. Perera, H.C. Liu, M. Buchanan, Z.R. Wasilewski, Uncooled infrared detectors for 3–5 μm and beyond, Appl. Phys. Lett. 93 (2) (2008) 021105.
[9] Y.F. Lao, P.K.D.D.P. Pitigala, A.G.U. Perera, H.C. Liu, M. Buchanan, Z.R. Wasilewski, K.K. Choi, P. Wijewarnasuriya, Light-hole and heavy-hole transitions for high-temperature long-wavelength infrared detection, Appl. Phys. Lett. 97 (9) (2010) 091104.
[10] Y.-F. Lao, A.G.U. Perera, Dielectric function model for *p*-type semiconductor inter-valence band transitions, J. Appl. Phys. 109 (10) (2011) 103528.
[11] M.R. Matthews, R.J. Steed, M.D. Frogley, C.C. Phillips, R.S. Attaluri, S. Krishna, Transient photoconductivity measurements of carrier lifetimes in an InAs/$In_{0.15}Ga_{0.85}As$ dots-in-a-well detector, Appl. Phys. Lett. 90 (10) (2007) 103519.
[12] Y.-F. Lao, S. Wolde, A.G. Unil Perera, Y.H. Zhang, T.M. Wang, H.C. Liu, J.O. Kim, T. Schuler-Sandy, Z.-B. Tian, S.S. Krishna, InAs/GaAs *p*-type quantum dot infrared photodetector with higher efficiency, Appl. Phys. Lett. 103 (24) (2013) 241115.
[13] Y.-F. Lao, S. Wolde, A.G. Unil Perera, Y.H. Zhang, T.M. Wang, J.O. Kim, T. Schuler-Sandy, Z.-B. Tian, S.S. Krishna, Study of valence-band intersublevel transitions in InAs/GaAs quantum dots-in-well infrared photodetectors, Appl. Phys. Lett. 104 (17) (2014) 171113.
[14] S.L. Chuang, Physics of Optoelectronic Devices, Wiley, New York, 1995.
[15] M.A. Cusack, P.R. Briddon, M. Jaros, Electronic structure of InAs/GaAs self-assembled quantum dots, Phys. Rev. B 54 (1996) R2300–R2303.
[16] H. Jiang, J. Singh, Strain distribution and electronic spectra of InAs/GaAs self-assembled dots: an eight-band study, Phys. Rev. B 56 (1997) 4696–4701.